VOL. 18, NO. 12, JUNE 2023 ISSN 1819-6608
ARPN Journal of Engineering and Applied Sciences

www.arpnjournals.com

INVESTIGATING THE EFFECT OF MOLASSES CONCENTRATIONS ON THE CHARACTERIZATION OF EVAPORATION BOAT WASTE FOR CRUCIBLE MATERIALS CANDIDATE

R. D. Widodo[1], R. Rusiyanto[1], A. Athoillah[1], R. Setiadi[1], A. Bahatmaka[1], F. B. Darsono[1], D. F. Fitriyana[1], J. P. Siregar[2], T. Cionita[3], R. Ismail[4], A. P. Bayuseno[4], A. P. Irawan[5], and NFDS Guterres[6]
[1]Department of Mechanical Engineering, Universitas Negeri Semarang, Kampus Sekaran, Gunungpati, Semarang, Indonesia
[2]Faculty of Mechanical and Automotive Engineering Technology, Universiti Malaysia Pahang, Pekan, Pekan, Malaysia
[3]Faculty of Engineering and Quantity Surveying, INTI International University, Nilai, Malaysia
[4]Department of Mechanical Engineering, Faculty of Engineering, Diponegoro University, Semarang, Jawa Tengah, Indonesia
[5]Faculty of Engineering, Universitas Tarumanagara, Jakarta Barat, Indonesia
[6]Department of Mechanical Engineering, Dili Institute of Technology, Ai-meti Laran Street, Dili, Timor-Leste
E-Mail: rahmat.doni@mail.unnes.ac.id

ABSTRACT

The crucible is a container wherein metallic materials are melted in order to generate new objects or alloys. Crucibles are typically formed of ceramic, graphite, silicon-carbide, and steel. Until now, there has been no study on the use of evaporation boat waste and molasses for the manufacture of crucibles. This study shows that molasses was used for binding the crucibles production formed from evaporation boats waste. The goal of this research was to ascertain how using molasses affected the properties of the crucible produced. Evaporation boat waste is made into powder (mesh 80) using a hammer mill. Molasses, evaporation boat waste powder and water with a certain concentration are mixed homogeneously using a mixer. The mixed material is put into a mold that has been adjusted to ASTM C1161-18, and then the compaction process is performed (20 MPa) to produce a green body. The resulting green body underwent a 16-hour drying time in an oven set at 100°C. Afterward, it was sintered for 240 minutes at 1150°C. The specimens in this study were characterized using XRD, SEM, density, hardness and 3-point bending tests. The test results show that molasses as a binder in the manufacture of crucible specimens does not result in the formation of a new crystalline phase. 5% molasses produced the best specimens. In specimens with 5% molasses, the density, hardness, flexural strength, and weight percentage (%) crystal phase of BN and TiB_2 were 2.25 g/cm^3, 61.6 HRA, 49.96 MPa, 67.5%, and 32.5%.

Keywords: crucible, evaporation boat waste, molasses

Manuscript Received 22 February 2023; Revised 16 August 2023; Published 30 August 2023

INTRODUCTIONS

Evaporation boats are material alloys used to produce thin aluminum films in decorative, plastic, glass, or food packaging applications in a high vacuum chamber [1]. The plastic metallization process is a process carried out by heating aluminum using evaporation boats to the melting point in a vacuum chamber so the atoms and molecules evaporate and stick to the surface of the plastic which moves at high speed and is then cooled rapidly so it crystallizes and forms a thin layer over the entire plastic layer [2]. This technology is widely used by the manufacturing industry that produces food packaging products such as PT 3M Indonesia. However, in its operation, industries engaged in this field always produce waste called evaporation boats waste (Figure 1). It is because of the lifespan of material evaporation boats which is only 15 hours [2]. After 15 hours, it is necessary to replace evaporation boats to maintain the effectiveness of the plastic metallization process. This is what causes the large volume of evaporation boat waste generated in the plastic metallization industry. 3M™ Evaporation Boat Dimet is made of Boron Nitride (BN) and Titanium Diboride (TiB_2) [3]. Both boron nitride (BN) and titanium diboride (TiB_2) exhibit exceptional levels of wear resistance, hardness, high-temperature stability, and melting point. These allow for the widespread use of BN and TiB_2 in industrial processes such as metal evaporation plating, wear-resistant coatings, and aerospace applications [4]–[6]. TiB_2-BN composite ceramics have good electrical conductivity, high wear resistance, and great machinability [5], [7]. Additionally, the mixture of TiB_2 and BN offers superior electrical conductivity and lubricity for molten metals. In the aluminum casting sector, TiB_2-BN composite ceramics are therefore frequently utilized [5].

Figure-1. Evaporation boats waste.

The large volume of evaporation boat waste shows the abundant availability of Boron Nitride and

Titanium Diboride materials. The content of Boron Nitride (BN) and Titanium Diboride (TiB_2) in evaporation boat waste is great potential for utilization and waste management in the near future. The utilization of waste for engineering applications and material synthesis has a positive impact on environmental sustainability [8]–[13]. The utilization of evaporation boat waste for crucible applications will reduce pollutants and will contribute to environmental sustainability. Aside from that, the cost of producing crucibles will be cheaper because the evaporation boat waste is affordable, easy to obtain, and available in large quantities.

The crucible is a container wherein metallic materials are melted in order to generate new objects or alloys. Traditionally, crucibles are manufactured from ceramic materials, which can sustain extremely high temperatures [14]. In this study, evaporation boat waste was used as the basic material for making crucibles with molasses as a natural binder. The industry that processes cane sugar produces molasses, which has 32% sucrose, 14% glucose, and 16% fructose as its major sugars. Sand molds, iron pellets, biofuel pellets, and heat-insulating bricks have all been made using molasses as a natural binder [15]–[20].

Typically, ceramic, graphite, silicon carbide, and steel are used to make crucibles [14]. To the best of our knowledge, there has not been any research on the use of evaporation boat waste and molasses in crucible production. Therefore, this work is the first report on the conversion of evaporation boat waste into crucibles using molasses as a binder. Scanning electron microscopy (SEM), X-ray powder diffraction (XRD) techniques, density, hardness, and flexural tests were used to characterize the formed crucible specimens.

MATERIALS AND METHODS

The evaporation boat waste investigated in this study was obtained from PT 3M Indonesia. Meanwhile, molasses was obtained from Putra Agro Lestari Store, Salatiga, Indonesia. The waste of evaporation boats is pulverized using a crusher machine and meshed using 80 mesh to produce evaporation boat waste powder (Figure-2).

Figure-2. Evaporation boats waste powder.

Figure-3 shows the X-ray diffraction (XRD) patterns test outcome that has been carried out by Rietveld refinement using the x'pert high score on evaporation boat waste powder. The content of Boron Nitride (BN) and Titanium Diboride (TiB_2) crystals in evaporation boat waste powder is 58.2% and 41.8%, respectively. Molasses and evaporation boat waste (powder) with a certain concentration (Table-1) are mixed homogeneously using a mixer. During the mixing process, water is added to as much as 15% of the total mixture of ingredients used.

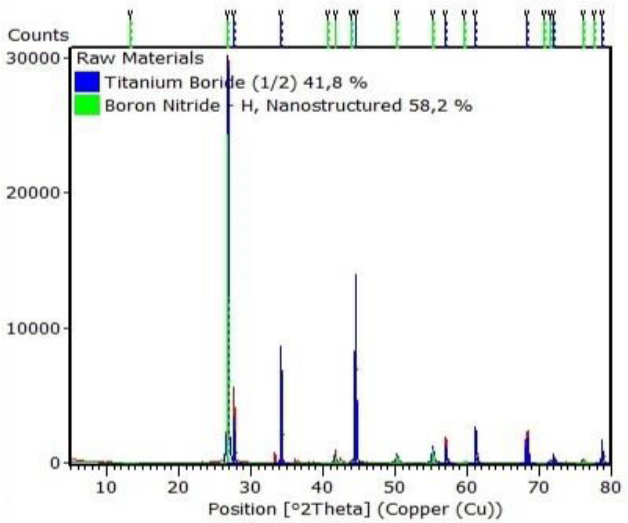

Figure-3. Result of XRD test on evaporation boats waste powder.

Table-1. Crucible specimen composition.

Specimens Code	Evaporation boat waste (powder) (wt.%)	Molasses (wt.%)
0%	100	0
5%	95	5
10%	90	10
15%	85	15
20%	80	20

The mixed material is put into a specimen mold that has been according to ASTM C1161-18, and then the compaction process is carried out using a hydraulic machine with a power of 20 MPa to produce a green body. The resulting green body was dried for 16 hours in an oven set to 100°C. In order to conduct the sintering procedure, a furnace is used to heat the green body specimen to 1150°C for 240 minutes. In this study, the sintering process was not carried out on the 15% and 20% specimens because the green body was not formed after compaction, as shown in Figure-4. This is due to the high water content of the material mixture, which prevents the compaction process from producing green bodies. The high water content causes all of the pores in the material mixture to fill with water, making it less compressible [21].

Figure-4. The compaction results were carried out on specimens with a molasses content of 15% and 20%.

The XRD, SEM, hardness, density, and 3-point bending test methods were used to characterize the study's findings. Using a scanning electron microscope (SEM) (JSM-6510, JEOL, Japan) at an exact 15 kV accelerating voltage, the surface morphology of the specimens was inspected. A high-sensitivity backscattered electron detector is installed on the bottom of the objective lens to create composition images, topography images, and shadow images. The crystal phase of specimens derived from evaporation boat waste and molasses was also examined using the Shimadzu XRD-7000. The High Score Plus program 3.0e was used to carry out the Rietveld analysis. The pseudo-Voigt function was used to describe the diffraction line profiles at the Rietveld refinement. The hardness test on the specimens formed in this study using the Rockwell hardness type A method with a force of 60 KgF.

The hardness testing process in this study refers to research conducted by Qi *et al.* (2019). In their research, the Rockwell hardness type A method was used to check the hardness of TiB_2-Fe-Co materials which had been heat treated at different temperatures (800°C-1200°C) [22]. The three-point bending test was performed to calculate the specimens' flexural strength and flexural modulus following the American Society for Testing and Materials (ASTM) C1161-18. An electronic density meter (DME 220 series) from Vibra Canada Inc., was used to conduct density testing.

RESULTS AND DISCUSSIONS

A graphic comparison of XRD test findings of the obtained specimens and evaporation boat waste is shown in Figure-5. TiB_2 and BN crystalline phases were found in evaporation boat waste and obtained specimens. The phase of BN crystals in evaporation boat waste and obtained specimens is commonly labeled as 2: 26.75, 41.61, 43.87, 50.16, 55.11, 59.54, 71.35, and 82.19 in accordance with JCPDS (Joint Committee on Powder Diffraction Standards) card number 01-073-2095 [23]. On other hand, the TiB_2 crystal phase is shown at 2θ: 27.69, 34.23, 44.51, 57.05, 61.18, 68.39, and 78.69 (JCPDS Card No. 85-2083) [24]. The XRD test findings revealed that only TiB_2 and BN diffraction peaks were found in all specimens, with no evidence of molasses or a possible reaction product. Furthermore, the results of the XRD test also showed that there were no impurities found in the evaporation boat waste powder and the resulting specimens. In this investigation, the use of molasses as a binder did not result in the formation of a new phase in all of the resulting specimens.

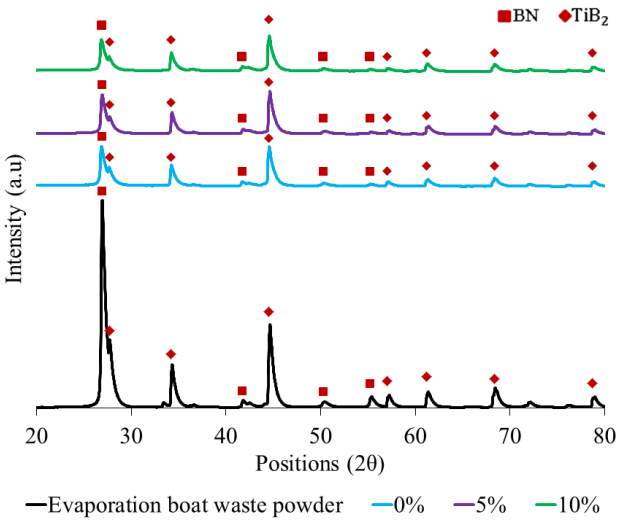

Figure-5. XRD Diffraction on the resulted specimen.

The findings in this test are in line with those of Qiu *et al.* (2021), who used hexagonal boron nitride (h-BN), lanthanum oxide (La_2O_3), alumina (Al_2O_3), and amorphous silica (SiO_2) as raw materials to create BN/La-Al-Si-O composite ceramics [25]. Only the hBN phase can be readily observed on the XRD graph, according to their study's findings. La_2O_3, Al_2O_3, SiO_2, and their potential reaction products' diffraction peaks, however, were left undiscovered. The crystalline phase found in all specimens is similar to the crystalline phase found in evaporation boat waste powder. The use of molasses and sintering temperature carried out in this study resulted in a decrease in the intensity of the TiB_2 and BN crystal phases which were shown at 2θ of 26.85, 27.69, 34.23, and 44.51. While the increase in the content of molasses as an adhesive in this study has an insignificant change in the intensity of TiB_2 and BN.

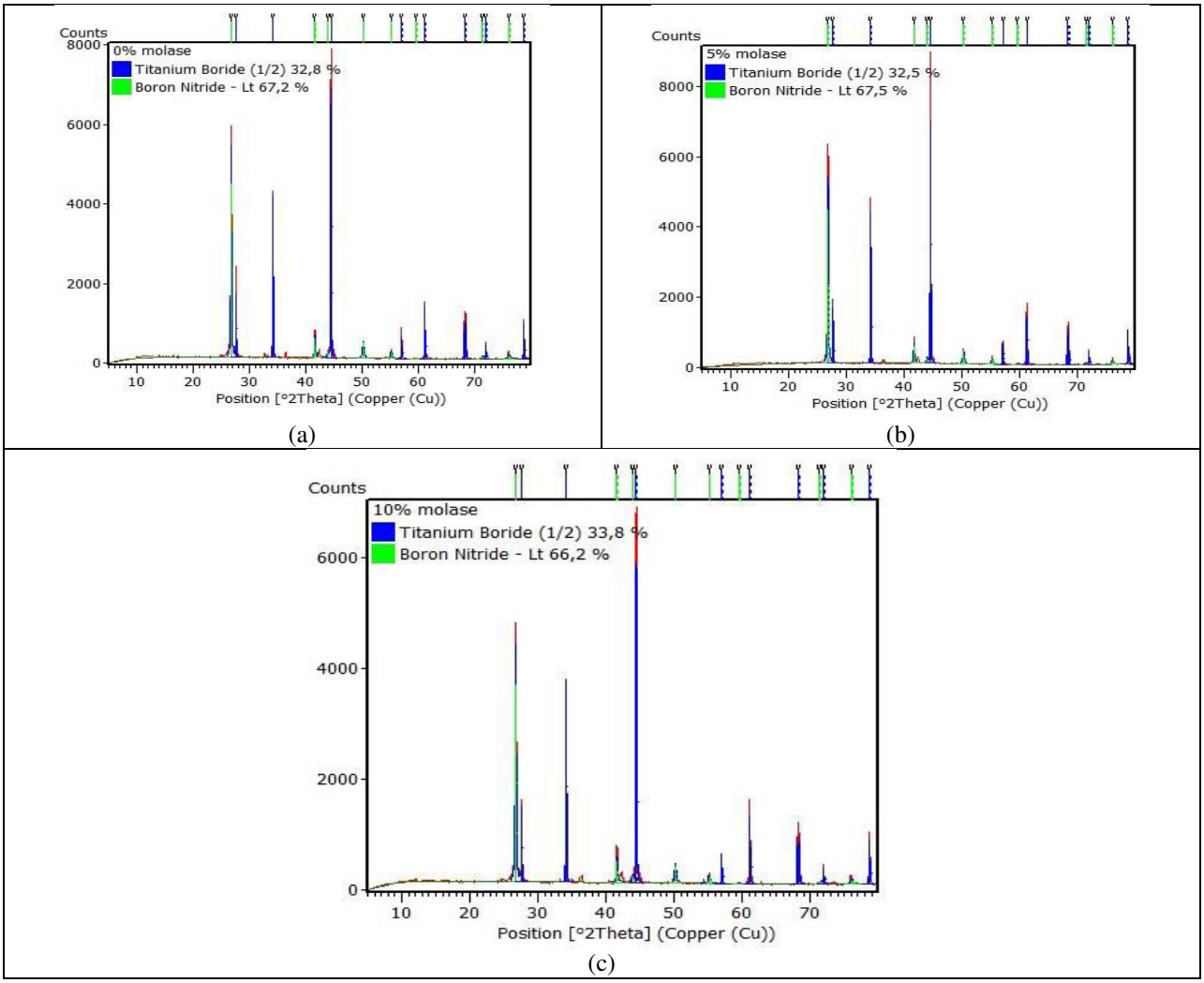

Figure-6. XRD diffraction patterns of specimens with various molasses concentrations (a) 0%, (b) 5%, and (c) 10%.

The evaporation boat waste powder has a higher intensity of BN and TiB2 crystals compared to the three specimens obtained. This is inseparable from the sintering process which is carried out at 1150°C. This is in line with research conducted by Petukhov *et al*. (2019) regarding the synthesis of Zr-ZrB2 composites by spark plasma sintering (SPS). In the XRD test they carried out, it was clear that the intensity of the BN crystal phase was quite high in the starting mixture. However, the SPS treatment at 900°C showed a significant decrease in the intensity of the BN crystal phase, and at a temperature of 1800°C, the peak of BN crystal was no longer found [26]. Research conducted by Angel et al. (2022) concluded that increasing the temperature and holding time of sintering resulted in a decrease in the intensity of the TiB_2 crystal phase on the XRD graph. This is due to the transformation of TiB_2 into TiB in the Ti-TiB_2 material sintering process [27].

Figure-3 (evaporation boat waste powder) and Figures-6a–6c, which show the results of a Rietveld analysis performed using High Score Plus software version 3.0e, indicate the weight in percent (%) of TiB_2 and BN crystals. The specimens with 5% molasses content had the largest weight percentage (%) of the BN crystal phase, which was 67.5%. Meanwhile, the highest Weight percentage (%) of crystal phase of TiB_2 was found in evaporation boat waste powder, which was 41.8%. TiB_2 and BN weight percentages (%) of their respective crystal phases for evaporation boat waste powder are 41.8% and 58.2%. The sintering treatment and the use of molasses in this study resulted in an increase in the Weight percentage (%) of the crystal phase of BN which reached the maximum value in the specimen with a molasses concentration of 5%. The weight percentage (%) of the crystal phase of BN decreases as the molasses concentration exceeds 5%. Different trends are shown in the percentage by weight (%) of the TiB_2 crystal phase. The weight percentage (%) of the TiB_2 crystal phase was reduced as a result of the sintering procedure and the usage of molasses in this investigation. The specimen with 5% molasses content had the lowest weight percentage (%) of the TiB_2 crystal phase, which was 32.5%.

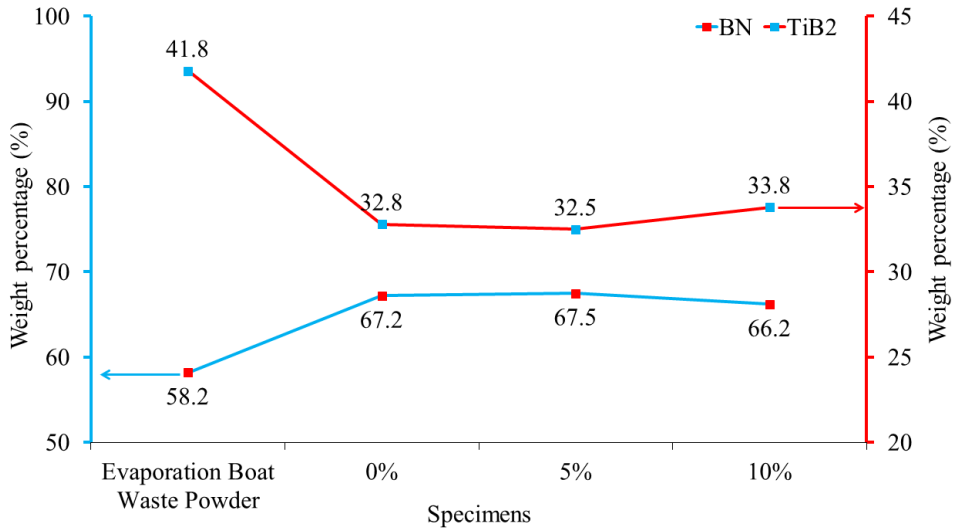

Figure-7. Comparison of weight percentage (%) of crystal phase on evaporation boat waste powder and obtained specimens.

Figure-7 compares the weight percentage (%) crystal phases of TiB_2 and BN crystals on the evaporation boat waste powder and obtained specimens. The results of this study indicated that there was a change in the weight percentage of BN and TiB2 crystals in evaporation boat waste powder after the manufacture of crucible specimens using molasses with different concentrations. In the evaporation boat waste powder, the weight percentage of BN and TiB2 crystals is 58.2% and 41.8%, respectively. After compaction (0% molasses) and sintering, the weight percentage values of BN and TiB2 crystals were 67.2% and 32.8%, respectively. This happened because BN and TiB_2 have differing sintering behaviors due to their different melting temperatures, which may result in the preferential compaction of one material over the other. The melting temperatures of TiB_2 and BN materials are 3225±20°C [28] and 2980°C [29], respectively. In general, BN is sintered more readily than TiB2, and as a result, BN crystals have a higher weight percentage (%) than TiB_2 crystals [30]. In this investigation, sintering was conducted at 1150°C, which allowed BN and TiB_2 crystals to grow and merge to form larger and more precisely defined crystals. The results of this study demonstrate that the weight percentage of BN crystals is higher than TiB_2, indicating that BN crystals grow more than TiB_2 crystals.

Figure-8 depicts SEM cross-sectional images of specimens from this study with varying molasses concentrations. This section's microstructure consisted of large crystalline grains and many crystals in flake shape (flaky crystals). The crystal with a flat structure is the BN phase, while the crystal with a granular structure is the TiB_2 phase which is dispersed among the BN crystal flakes. The flake crystals were more clearly visible with increasing molasses concentration, especially at 5% molasses concentration. The findings in this study have the same phenomenon as the microstructure of TiB_2-BN-SiC composite ceramics in the study of Tian *et al*. (2022) [5]. In addition, their findings also demonstrated that the granular crystals (TiB_2 and SiC) were uniformly dispersed in flake-shaped BN crystals.

The similar conclusion was also obtained from SEM investigations of the morphology of BN and TiB2 crystals carried out by Popov *et al*. (2022) [30] and Peighambardoust *et al*. (2021) [31].

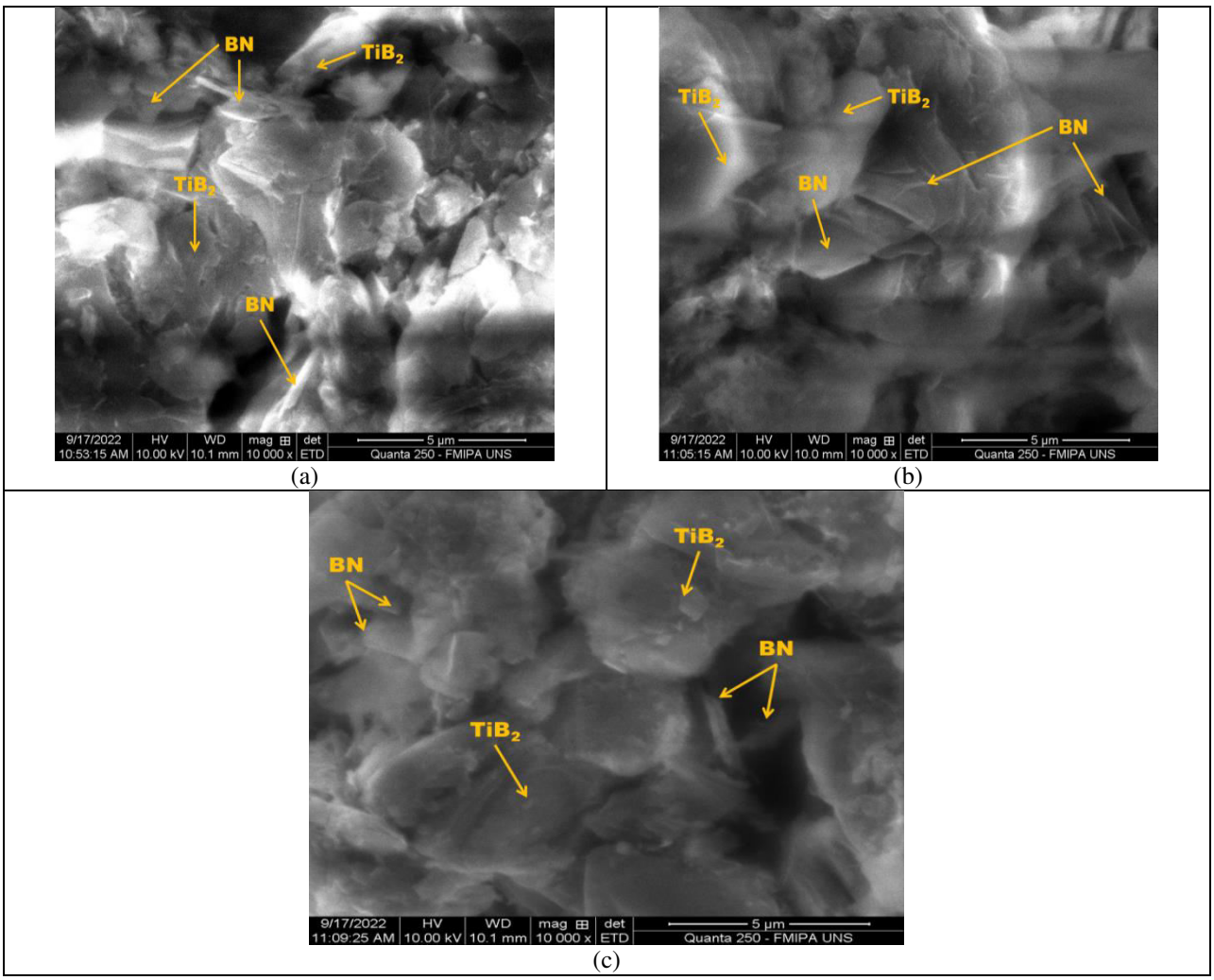

Figure-8. SEM images of specimens with various molasses concentrations (a) 0%, (b) 5%, and (c) 10% with 10000 magnifications.

The specimen with a molasses concentration of 10% produced the lowest density (2.21 g/cm^3) compared to other specimens (Figure-9). The specimen with a 5% molasses concentration produced the highest density of 2.25 g/cm^3. Meanwhile, the specimen with 0% molasses concentration resulted in a density of 2.23 g/cm^3. In this study, increasing the concentration of molasses from 0% to 5% had a density increase. However, the density of the specimen decreased when the molasses concentration approached 5%. These findings are similar to those of Utchariyajit *et al.* (2019), who produced briquettes out of Palmyra palm trash using molasses as a binder. According to their research, the densest briquettes were those with 5% weight-to-weight molasses, followed by those with 10% and 15% w/w molasses.

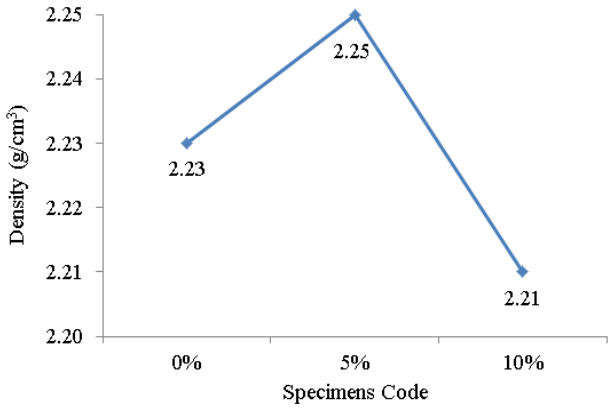

Figure-9. Density of specimens with different molasses concentrations.

As the molasses content of briquettes decreases, the density of the briquettes increases [32]. Syahfitri *et al.* (2022) demonstrated that the composite lightweight roof tile density decreased as the molasses content increased. Molasses content of 10% will produce lightweight roof tile composite with the highest density [33]. The

investigation carried out by Jiménez *et al*. (2022) likewise produced results that were similar. A composite with a high density is produced when the molasses concentration is 2%. The composite density decreases as molasses concentration increases [34].

The density of the specimen increased as the molasses content was raised from 0% to 5%. This is impacted by the increase in binder concentration, which makes pores to close up and a stronger link to form between the waste from evaporation boats and the molasses binder. The increase in the concentration of the binder causes the grain size to increase due to the increase in particle coalescence, so that the porosity decreases and the mechanical properties increase [35], [36]. The findings of this study showed that the sample to which 5% molasses had been added generated the specimen with the highest density. Effective binder burnout can increase the density of the sintered body, but insufficient removal can lead to flaws including black coring, cracking, bloating, and the emergence of blocked pores. They are detrimental to the sintered material's mechanical properties [37].

The density of Cf/C-SiC composites steadily rises with an increase in binary binder content, according to Liu et al. (2022) [38]. On the other hand, the density of the specimen decreased when the molasses content was increased from 5% to 10%. Yu et al. (2010) discovered that the porosity of porous silicon nitride ceramics is influenced by the binders' number ratio. The higher the concentration of binder, the resulting porosity increases. The pores from the sintered body are mostly derived from the leftover micro-space of the organic processing aids after organic binder burnout in the green body [39]. Furthermore, research conducted by Ayorinde *et al.* (2013) showed a decrease in particle density with an increase in molasses concentration [40].

The effect of molasses concentration on hardness and density is shown in Figure-10. The highest hardness obtained in specimens using molasses with a concentration of 5% is 62 HRA. The specimens using molasses with a concentration of 10% produced the lowest hardness of 52 HRA. Meanwhile, the specimens without molasses (0%) produced a flexural strength of 58 HRA. In general, a material's hardness tends to rise as its density increases [41]–[44].

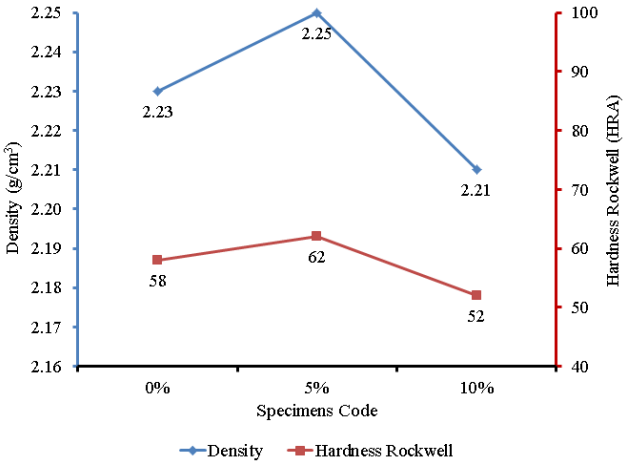

Figure-10. Hardness and density of specimens with different molasses concentrations.

This is because a material with a higher density typically has a more compact and organized structure that can withstand deformation and preserve its shape when subjected to external forces. Raising the content of molasses from 0% to 5% led to an increase in density, followed by an increase in Rockwell hardness. Increasing the percentage of molasses from 5% to 10% caused a decrease in density values, followed by a decrease in Rockwell hardness values. This study's findings are consistent with research conducted by Babapoor *et al.* (2018). Their research revealed a linear correlation between the density and hardness of titanium carbide treated with spark plasma sintering (SPS). Raising the temperature of SPS from 1800°C to 1900°C led to an increase in relative density followed by an increase in Vickers hardness. However, as the temperature is increased from 1900 °C to 2000 °C, the relative density value decreases, which is followed by a reduction in the Vickers hardness value [45].

The effect of molasses concentration on flexural strength and density is shown in Figure-11. The highest flexural strength obtained in specimens using molasses with a concentration of 5% is 49.96 MPa. The specimens using molasses with a concentration of 10% produced the lowest flexural strength of 28.35 MPa. Meanwhile, the specimens using molasses with a concentration of 0% produced a flexural strength of 37.01 MPa. The results of the study done by Ahinöz *et al*. (2022) corroborate the conclusions in this study. Their findings indicated that adding up to 35% more molasses increased the flexural strength of the composite pine cone material. Molasses content greater than 35% (40%, 45%, and 47.5%) caused a decrease in flexural strength [46].

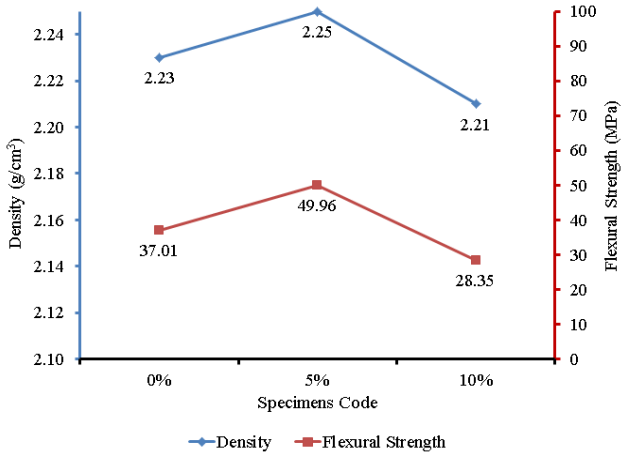

Figure-11. Flexural strength and density of specimens with different molasses concentrations.

In general, a material's mechanical properties decrease substantially as its density decreases [47], [48]. The study's findings also make it abundantly clear that the specimen's flexural strength increases as density rises. The use of molasses with a concentration of 5% produces specimens with the highest flexural strength. Furthermore, flexural strength decreased with increasing molasses concentration (10%). This happened because the density of the specimen decreased with the use of molasses with a concentration of more than 5%. Increased flexural strength reflects the specimen's ability to absorb more energy, extend the path of crack propagation, and increase plastic deformation. Consequently, the surface fracture energy and strength of the specimen are enhanced [49].

These findings are consistent with the Zang *et al.* (2018) investigations [50]. Their findings demonstrated that the flexural strength of porous ceramics based on Si_3N_4 rise dramatically when the density of the resulting specimens increased due to a reduction in porosity. These results are also supported by research on the manufacture of composites from polyurethane and fly ash conducted by Shivakumar *et al.* (2019).

The higher the concentration of fly ash used, the higher the density of the composite. The flexural strength of a composite material increases in direct proportion to its density [51]. Manni *et al.* (2019) discovered that the density of porous red ceramics (class BIII) decreased as the concentration of coffee waste increased. Additionally, as density drops, the flexural strength of the porous red ceramics also declines [52].

CONCLUSIONS

The manufacture and characterization of crucible specimens made from evaporation boats waste using molasses as a binder has been successfully carried out. A new crystal phase is not created when molasses is used as a binder to create crucible specimens from evaporation boat waste. This is evidenced by the XRD test which only found TiB_2 and BN crystal phases in all the specimens produced. This study found that adding more molasses as an adhesive had no discernible impact on the amount of TiB_2 and BN. The SEM image on the crucible specimen shows the crystal with a flat structure is the BN phase, while the crystal with a granular structure is the TiB_2 phase which is dispersed among the BN crystal flakes. The use of molasses as an adhesive has been shown to have a positive impact on the hardness, flexural strength and density of crucible specimens. The use of molasses with a concentration of 5% resulted in crucible specimens with the highest hardness (62 HRA), flexural strength (49.96 MPa) and density (2.25 g/cm^3) compared to other specimens. This happens because the increase in the concentration of the molasses causes the grain size to increase due to the increase in particle coalescence, so that the porosity decreases and the mechanical properties increase.

ACKNOWLEDGMENTS:

The authors are humbly proclaiming their gratitude to the Faculty of Engineering at Universitas Negeri Semarang (UNNES) for the respectable award, "Penelitian Pengembangan" Research Grant for the year 2022.

CONFLICTS OF INTEREST

The authors declare that they have no conflict of interest.

REFERENCES

[1] K. Gürcan Bayrak, F. Agyurek, E. Ayas, Y. Göncü, and N. Ay. 2014. Obtaining of TiB2 Powder from Evaporation Boat Waste.

[2] J. Bayus. 2015. Environmental Life Cycle Comparison of Aluminum-based High Barrier Flexible Packaging Laminates.

[3] 3M Advanced Materials, "3M Evaporation Boats," pp. 1-2, 2015.

[4] Q. He *et al.* 2021. Microstructure and mechanical properties of TiN-TiB2-hBN composites fabricated by reactive hot pressing using Tin-B mixture. Materials (Basel). 14(23).

[5] H. W. and W. W. Shi Tian, Zelin Liao, Wenchao Guo, Qianglong He. 2022. Effects of theTiB2-SiC Volume Ratio and Spark Plasma Sintering Temperature on the Properties and Microstructure of TiB2-BN-SiC Composite Ceramics. Crystals. 12(29): 1-13.

[6] B. Song, W. Yang, X. Liu, H. Chen, and M. Akhlaghi. 2021. Microstructural characterization of TiB2–SiC–BN ceramics prepared by hot pressing. Ceram. Int., 47(20): 29174-29182.

[7] E. E. Songül and I. Duman. 2020. Modeling of TiB2–BN Composites as Cathode Materials for Aluminum Electrolysis Cell. in Green Energy and Technology. pp. 817-841.

[8] A. Bayu *et al*. 2020. Isotherm adsorption characteristics of carbon microparticles prepared from pineapple peel waste. Commun. Sci. Technol. 5(1): 31-39.

[9] A. B. D. Nandiyanto *et al*. 2021. The effects of rice husk particles size as a reinforcement component on resin-based brake pad performance: from literature review on the use of agricultural waste as a reinforcement material, chemical polymerization reaction of epoxy resin, to experiments," Automot. Exp. 4(2): 68-82.

[10] A. B. D. Nandiyanto *et al.* 2020. Synthesis of carbon microparticles from red dragon fruit (Hylocereus undatus) peel waste and their adsorption isotherm characteristics. Molekul. 15(3): 199-209.

[11] D. F. Fitriyana, H. Suhaimi, Sulardjaka, R. Noferi, and W. Caesarendra. 2020. Synthesis of Na-P Zeolite from Geothermal Sludge. Springer Proc. Phys. 242: 51-59.

[12] D. F. Fitriyana, R. Ismail, Y. I. Santosa, S. Nugroho, A. J. Hakim, and M. Syahreza Al Mulqi. 2019. Hydroxyapatite Synthesis from Clam Shell Using Hydrothermal Method : A Review. 2019 Int. Biomed. Instrum. Technol. Conf. IBITeC 2019, pp. 7–11, Oct. 2019.

[13] R. Ismail *et al.* 2021. The potential use of green mussel (Perna Viridis) shells for synthetic calcium carbonate polymorphs in biomaterials. J. Cryst. Growth, p. 126282.

[14] K. Arzt. 2022. What Is A Crucible ?

[15] N. P. Carnaje, R. B. Talagon, J. P. Peralta, K. Shah and J. Paz-Ferreiro. 2018. Development and characterisation of charcoal briquettes from water hyacinth (Eichhornia crassipes)-molasses blend. PLoS One. 13(11): e0207135.

[16] P. K. S. Bhide, Jayesh Darshane, D. Shinde, Sudhanshu Dhokale, P. Deshmukh, Yash desai. 2017. Effect of Sugarcane Molasses on Compressive Strength and Workability of Fly Ash Mixed Concrete. Int. J. Sci. Res. Sci. Eng. Technol. 3: 607-612.

[17] A. Benk and A. Coban. 2012. Possibility of producing lightweight, heat insulating bricks from pumice and H3PO4- or NH4NO3-hardened molasses binder. Ceram. Int. 38: 2283-2293.

[18] A. Kotha, A. Patra, and D. S. Karak. 2019. Effect of molasses binder on the physical and mechanical properties of iron ore pellets. Int. J. Miner. Metall. Mater. 26: 41-51.

[19] T. Wang *et al.* 2019. Effect of molasses binder on the pelletization of food waste hydrochar for enhanced biofuel pellets production. Sustain. Chem. Pharm. 14: 100183.

[20] B. Ibrahim, Y. Tijjani, I. A. Rafukka and M. U. Suleiman. 2014. Application of molasses as a binder in sand mold operation. Appl. Mech. Mater. 660: 301-305.

[21] M. F. Nawaz, G. Bourrié, and F. Trolard. 2013. Soil compaction impact and modelling. A review. Agron. Sustain. Dev. 33(2): 291-309.

[22] L. Qi, T. Han and Y. Zhang. 2019. Electrostatic precipitability of TiB2-Fe-Mo-Co ceramic-metal composites. J. Alloys Compd. 778: 507-513.

[23] S. Yuan et al. 2016. Pure &crystallized 2D Boron Nitride sheets synthesized via a novel process coupling both PDCs and SPS methods. Sci. Rep. 6: 20388.

[24] X. Huang, S. Sun, G. Tu, S. Lu, K. Li, and X. Zhu. 2017. The Microstructure of Nanocrystalline TiB_2 Films Prepared by Chemical Vapor Deposition. Mater. (Basel, Switzerland). 10(12).

[25] B. Qiu *et al.* 2021. Microstructural evolution of h-BN matrix composite ceramics with La-Al-Si-O glass phase during hot-pressed sintering. J. Adv. Ceram. 10(3): 493-501.

[26] O. S. Petukhov, A. V Ragulya, and H. Y. Borodianska. 2019. Synthesis of the ZrN–ZrB2 Composite by Spark Plasma Sintering. Powder Metall. Met. Ceram. 58(7): 416-430.

[27] D. A. Angel, T. Miko, F. Kristaly, M. Benke, Z. Gacsi, and G. Kaptay. 2022. Complex Avrami kinetics of TiB2 transformation into TiB whiskers during sintering of Ti-TiB2 nanocomposites. J. Alloys Compd. 894: 162442.

[28] R. G. Munro. 2000. Material Properties of Titanium Diboride. J. Res. Natl. Inst. Stand. Technol. 105(5): 709-720.

[29] L. Tang, B. Lin, B. Zhang, D. Zhang, Y. Gong and N. Xiong. 2022. Research Status of Titanium Diboride High Temperature Ceramics. J. Phys. Conf. Ser. 2200(1).

[30] O. Popov *et al.* 2021. Reaction Sintering of Machinable TiB2-BN-C Ceramics with In-Situ Formed h-BN Nanostructure. Nanomaterials. 12(8).

[31] N. S. Peighambardoust, Ç. Çevik, T. Assar, S. Jung, S. Y. Lee and J. H. Cha. 2021. Pulsed electric current sintering of TiB2-based ceramics using nitride additives. Synth. Sinter. 1(1): 28-33.

[32] K. Utchariyajit, V. Panprasert, L. Chayawat, W. Jungthanasombat, P. Janprom and M. Choatchuang. 2019. Physical properties and calorific value of briquettes produced from Palmyra palm waste with molasses binder. IOP Conf. Ser. Mater. Sci. Eng. 639(1).

[33] A. Syahfitri *et al.* 2022. Conversion of agro-industrial wastes of sorghum bagasse and molasses into lightweight roof tile composite. Biomass Convers. Biorefinery.

[34] J. E. Jiménez, C. M. Fontes Vieira, and H. A. Colorado. 2022. Composite Soil Made of Rubber Fibers from Waste Tires, Blended Sugar Cane Molasses, and Kaolin Clay. Sustain. 14(4): 1-15.

[35] P. Thapa, J. Tripathi and S. H. Jeong. 2019. Recent trends and future perspective of pharmaceutical wet granulation for better process understanding and product development. Powder Technol. 344: 864-882.

[36] A. Khan. 2021. Prediction of quality attributes (mechanical strength, disintegration behavior and drug release) of tablets on the basis of characteristics of granules prepared by high shear wet granulation. PLoS One. 16(12): e0261051.

[37] D. Mohanty. 2011. Effect of Holding Time on Binder Burnout, Density and Strength of Green and Sinterd Alumina Samples. NATIONAL INSTITUTE OF TECHNOLOGY ROURKELA, INDIA.

[38] Y. Liu et al. 2022. Binary Binder for Cf/C-SiC Composites with Enhanced Mechanical Property. Mater. (Basel, Switzerland). 15(8).

[39] J. Yu, H. Wang, J. Zhang, D. Zhang and Y. Yan. 2010. Gelcasting preparation of porous silicon nitride ceramics by adjusting the content of monomers. J. Sol-Gel Sci. Technol. 53(3): 515-523.

[40] J. O. Ayorinde, A. O. Itiola and M. A. Odeniyi. 2013. Effects of excipients and formulation types on compressional properties of diclofenac. Acta Pol. Pharm. - Drug Res. 70(3): 557-566.

[41] A. H. Dawam Abdullah and S. Nasution. 2018. Effect of Heating Time to Density, Hardness, and Resistivity Againt Fungus of Yellow Bamboo (Bambusa Vulgaris Var Schard. Vitata). IOP Conf. Ser. Mater. Sci. Eng. 299(1).

[42] A. Nikmah, D. Izak Rudyardjo, J. Ady and A. Taufiq. 2019. Studies on Density, Corrosion Rate and Hardness Characteristics of Stainless Steel Implanted by Nitrogen Ion. IOP Conf. Ser. Mater. Sci. Eng. 515(1).

[43] J. P. Cabral, B. Kafle, M. Subhani, J. Reiner and M. Ashraf. 2022. Densification of timber: a review on the process, material properties, and application. J. Wood Sci. 68(1): 20.

[44] M. Madej, B. Leszczyńska-Madej and D. Garbiec. 2022. Effect of Sintering Temperature and Iron Addition on Properties and Microstructure of High Speed Steel Based Materials Produced by Spark Plasma Sintering Method," Materials (Basel). 15(21).

[45] A. Babapoor, M. S. Asl, Z. Ahmadi and A. S. Namini. 2018. Effects of spark plasma sintering temperature on densification, hardness and thermal conductivity of titanium carbide. Ceram. Int. 44(12): 14541-14546.

[46] M. Şahinöz, H. Y. Aruntaş and M. Gürü. 2022. Processing of polymer wood composite material from pine cone and the binder of phenol formaldehyde/PVAc/molasses and improvement of its properties. Case Stud. Constr. Mater. 16: e01013.

[47] Q. Wu, W. Miao, Y. Zhang, H. Gao and D. Hui. 2020. Mechanical properties of nanomaterials: A review. Nanotechnol. Rev. 9(1): 259-273.

[48] H. Laoubi, M. Bederina, A. Djoudi, A. Goullieux, R. M. Dheilly, and M. Queneudec. 2018. Study of a New Plaster Composite Based on Dune Sand and Expanded Polystyrene as Aggregates. Open Civ. Eng. J. 12(1): 401-412.

[49] D. F. Fitriyana *et al*. 2022. The effect of hydroxyapatite concentration on the mechanical properties and degradation rate of biocomposite for biomedical applications. IOP Conf. Ser. Earth Environ. Sci. 969(1): 012045.

[50] X. Zhang *et al.* 2019. Porous Si3N4-based ceramics with uniform pore structure originated from single-shell hollow microspheres. J. Mater. Sci. 54(6): 4484-4494.

[51] K. N. Shivakumar, W. H. Brown and K. A. Imran. 2019. Fly Ash Composites, A Step toward Pond Ash Composites. Coal Combust. Gasif. Prod., no. June.

[52] A. Manni, A. El Haddar, I. E. El Amrani El Hassani, A. El Bouari and C. Sadik. 2019. Valorization of coffee waste with Moroccan clay to produce a porous red ceramics (class BIII). Bol. la Soc. Esp. Ceram. y Vidr. 58(5): 211-220.